ESA Climate Change Initiative Plus (CCI+)

Product User Guide version 3 (PUGv3) for the University of Leicester Full-Physics XCO_2 TanSat data product (CO2_TAN_OCFP v1.2)

-

The University of Leicester Full-Physics Retrieval Algorithm for the retrieval of XCO_2 from TanSat

for the Essential Climate Variable (ECV) Greenhouse Gases (GHG)

Version 3, revision 1

14th February 2022

Written by
Simon Preval, Dongxu Yang, and Hartmut Boesch
Department of Physics and Astronomy, National Centre for Earth Observation, and Space Park Leicester
University of Leicester
Leicester
United Kingdom
Document history:

Version	Revision	Date	Status	Description/Comments
1	0	26/10/2019	Submitted	New document.
1	1	20/12/2019	Revision	Corrections in response to ESA comments.
2	0	23/11/2020	Submitted	Update for first global product.
2	1	10/02/2021	Revision	Corrections in response to ESA comments.
3	0	26/11/2021	Submitted	Update for CO2_TAN_OCFP v1.1 global product.
3	1	14/02/2022	Submitted	Updated PUG document correcting errors in previous CO2_TAN_OCFP v1.1 product, and creation of new product CO2_TAN_OCFP v1.2.

Table of Contents

1 Summary 5

2 Introduction 6

2.1 The ACGA/TanSat Instrument 6

2.2 The University of Leicester Full-Physics XCO_2 Product 6

2.3 Validation 6

3 Product Description 8

3.1 Product Content and Format 8

3.2 Quality Flags and Metadata 8

3.3 Bias correction 10

3.4 Data Usage 10

3.5 Tools for Reading the Data 10

3.6 Known Limitations and Issues 10

3.7 Global data plots 11

3.8 Data file content 14

4 Acknowledgement 16

5 References and Further Reading 16

List of Tables

Table 1. Product quality filter; retrievals that satisfy these criteria are marked as good. .9
Table 2. Bias correction coefficients. The coefficient for each row from left to right indicate the footprint. 10
Table 3. Common variables for the CO2_TAN_OCFP data product. 14
Table 4. Additional variables for the CO2_TAN_OCFP data product. 15

List of figures

Figure 1: Comparison of the CO2_TAN_OCFP V1 (CRDP#5, orange) with the TCCON XCO_2 (blue, overpass mean) between March 2017 and May 2018. The overpass-mean from TanSat is indicated with large orange solid circles with error bars indicating the standard deviation, and small orange points show individual soundings. We plot all measurements that satisfy the co-location criteria of an overpass. 7
Figure 2: Comparison of individual retrieved XCO_2 from TanSat with the overpass mean of TCCON XCO_2 for the time period of March 2017 to May 2018 across all 20 TCCON sites. Each TCCON site is given by different colour and symbol. Statistics for mean bias and RMSE (calculated by averaging the bias and RMSE of each site) are given along with the correlation coefficient. 8
Figure 3: Global monthly median XCO_2 concentrations as a function of longitude and latitude for March 2017 – May 2018 as observed by TanSat. The soundings have been bias-corrected and filtered as per Table 1. 12
Figure 4: Standard deviation ($\boldsymbol{\sigma XCO2}$) of XCO_2 concentrations as a function of longitude and latitude for March 2017 – May 2018 as observed by TanSat. The soundings have been bias-corrected and filtered as per Table 1. 13

1 Summary

This document is the Product User Guide Version 3 (PUGv3), which is a deliverable of the ESA project GHG-CCI+. The GHG-CCI+ project is a continuation of the ESA Climate Change Initiative (CCI) project. The GHG-CCI+ project will deliver the Essential Climate Variable (ECV) Greenhouse Gases (GHG). State-of-the-art retrieval algorithms for remote sensing of the GHG and the ECV will be developed further in the frame of this project. Multi-year carbon dioxide (CO_2) data sets will be generated and validated.

The Atmospheric Carbon-dioxide Grating Spectrometer ACGS on TanSat will be used to produce the core GHG-ECV products (XCO_2). The instrument measures Near Infra-Red (NIR) and Short Wave Infra-Red (SWIR) spectra of reflected solar radiation which are sensitive to CO_2 concentration changes close to Earth's surface. Consequently, they offer information on regional surface fluxes. The accuracy requirements for such an application are demanding. This document describes the University of Leicester Full-Physics XCO_2 (CO2_TAN_OCFP v1.2) data product so that it will be clear for the user how to use the products. The description includes quality flags and metadata, data format, product grid and geographical projection, known limitations, available tools for decoding and interpreting the data. The product described in this user guide supersedes that described in PUGv3 (CO2_TAN_OCFP v1.1) as it corrects an error in the assignment of the quality flags and filtering in this dataset. This error is not present in CRDP#5, meaning the validation presented in PUGv1 is still valid and applies to this data version.

2 Introduction

2.1 The ACGA/TanSat Instrument

The Chinese Global Carbon Dioxide Monitoring Scientific Experimental Satellite (TanSat) is the first Chinese CO_2 monitoring satellite, launched on 22 December 2016. TanSat provides global measurements of total column CO_2 from its NIR/SWIR band. The mission aims are to monitor the column density of CO_2 precisely and frequently worldwide, to study the absorption and emission levels of CO_2 on a regional scale over a certain period of time, and to develop and establish advanced technologies that are essential for precise CO_2 observations /Liu et al., 2018/.

As the primary instrument onboard TanSat, Atmospheric Carbon dioxide Grating Spectrometer (ACGS) is designed to measure NIR/SWIR backscattered sunlight in the molecular oxygen (O_2) A band (0.76 µm) and two CO_2 bands (1.61 and 2.06 µm). Total column CO_2 is mainly determined from measurements of its absorption lines in the weak band (1.61 µm). Sunlight is significantly scattered and absorbed by air molecules and suspended particles (e.g., clouds and aerosols), which would result in serious errors in CO_2 retrievals. Consequently, more information from cloud and aerosol measurements is required for the CO_2 retrieval to correct the light path. This is acquired by the O_2 A band that provides information on altitude and total amount (optical depth) of aerosols and clouds due to almost constant and stable O_2 concentrations in the atmosphere. In comparison, the interference from water vapour absorption is relatively weak. However, the CO_2 weak band is spectrally far away from the O_2 A band, and aerosol and cloud optical properties depend on wavelength. Thus, it is also necessary to constrain this spectral variation which is one of the purposes of the strong CO_2 band. The strong CO_2 band also provides information on water vapour and temperature, which reduces impacts from uncertainties in these parameters.

The design of the optical layout of ACGS and the specifications of instrument optical parameters can be found in a previous study /Lin et al., 2017/. The footprint on the ground is 2 km × 2 km in the nadir mode with 9 footprints in each swath and a total width of the field of view (FOV) of ~18 km at nadir. The first global carbon dioxide maps produced from TanSat measurements have been produced by the IAPCAS (Institute of Atmospheric Physics Carbon dioxide retrieval Algorithm for Satellite remote sensing) TanSat algorithm /Yang et al., 2018/, and then verified (~2.11 ppm of precision in 8 TCCON sites average) by TCCON Total Carbon Column Observing Network measurements /Liu et al., 2018/.

2.2 The University of Leicester Full-Physics XCO_2 Product

The Leicester CO2_TAN_OCFP v1.2 product is retrieved from ACGS/TanSat NIR and SWIR spectra using the University of Leicester (UoL) Full-Physics Retrieval Algorithm modified for the use of TanSat spectra. The retrieval algorithm uses an iterative retrieval scheme based on Bayesian Optimal Estimation Method (OEM) to retrieve a set of atmospheric, surface and instrument parameters, referred to as the state vector, from measured spectral radiances /Boesch et al., 2011; Connor et al., 2008/. The forward model, used to relate the state vector to the measured radiances, includes the LIDORT /Spurr et al., 2008/ and TWOSTR /Spurr et al., 2011/ radiative transfer models combined with a fast 2 orders of scattering vector radiative transfer code /Natraj et al., 2008/. In addition, we use the low-streams interpolation functionality of the code /O'Dell et al., 2010/ to accelerate the radiative transfer component of the retrieval algorithm. The TanSat XCO_2 data is produced by using the O_2 A band together with the weak CO_2 band.

2.3 Validation

Validation of our retrieved XCO_2 has been performed against TCCON /Wunch et al., 2013/, a global network of ground-based high-resolution Fourier transform spectrometers recording direct solar spectra in the NIR/SWIR spectral region, itself validated against aircraft measurements. Note that validation of the v1.2 product is performed using the CRDP#5 data release. As mentioned in the Executive Summary, an error was detected in the CO2_TAN_OCFP v1.1 data, where the data was incorrectly filtered, and quality flags were not assigned correctly. This error is corrected in the present data release (CO2_TAN_OCFP v1.2).

Figure 1 shows retrieved TanSat XCO_2 compared to 20 TCCON sites for the period March 2017 to May 2018, using the TCCON data (GGG2015, retrieved from TCCON data archive on 1 June 2019), and co-

located spatially and temporally by selecting TanSat soundings only in a ±3º latitude/longitude box around the TCCON site, and ± 1 hours of each TCCON measurement.

Overall, good agreement between TCCON and CO2_TAN_OCFP v1 (CRDP#5) is found, with the magnitude and phase of the seasonal cycle being well captured over a variety of sites /Yang et al., 2020/. Figure 2 shows the total correlation across all sites with individual soundings, with a correlation coefficient of 0.82 and a RMSE of 1.78 ppm.

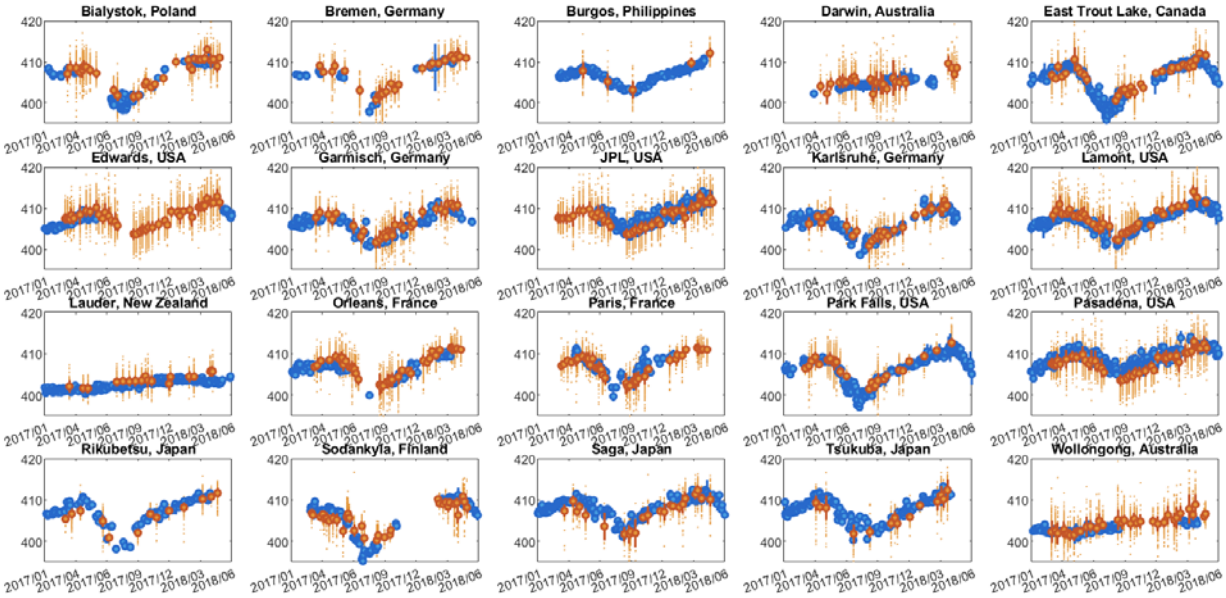

Figure 1: Comparison of the CO2_TAN_OCFP v1 (CRDP#5, orange) with the TCCON XCO_2 (blue, overpass mean) between March 2017 and May 2018. The overpass-mean from TanSat is indicated with large orange solid circles with error bars indicating the standard deviation, and small orange points show individual soundings. We plot all measurements that satisfy the co-location criteria of an overpass.

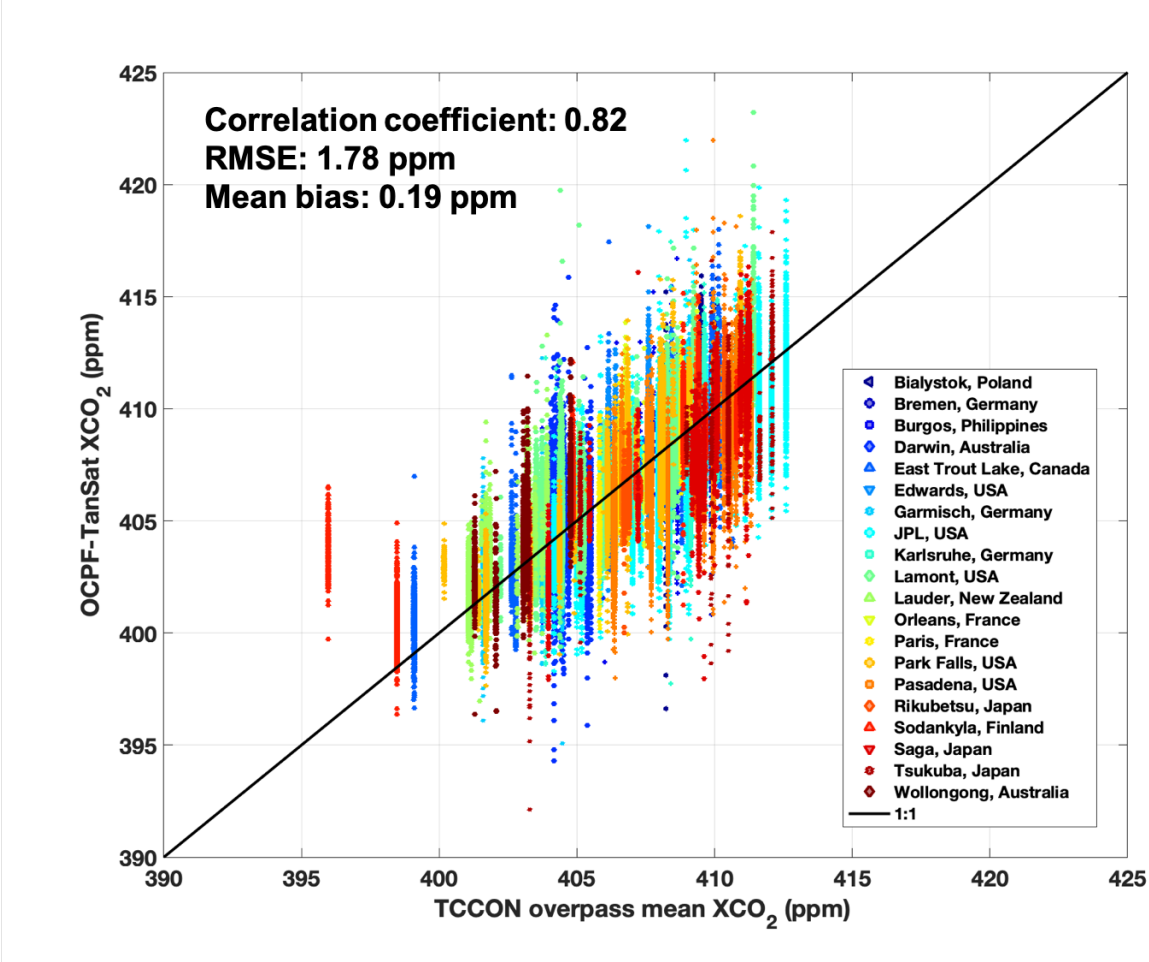

Figure 2: Comparison of individual retrieved XCO_2 from TanSat with the overpass mean of TCCON XCO_2 for the time period of March 2017 to May 2018 across all 20 TCCON sites. Each TCCON site is given by different colour and symbol. Statistics for mean bias and RMSE (calculated by averaging the bias and RMSE of each site) are given along with the correlation coefficient.

3 Product Description

3.1 Product Content and Format

XCO_2 data are stored in the NetCDF format, with each daily file containing soundings around each TCCON site. Table 3 provides a description of the variables common to all ESA GHG-CCI data products, and all necessary parameters to make use of the data (e.g. a-priori data, column averaging kernels, quality information, etc.). Table 4 contains additional product-specific variables, such as instrument flags and important ancillary retrieval information.

3.2 Quality Flags and Metadata

The data product contains an "xco2_quality_flag" variable, indicating whether the data has passed our quality checks. In normal use, only data with an xco2_quality_flag equal to 0 should be used. Only TanSat soundings that pass the cloud screen (i.e. apparent surface pressure difference between O_2-A band retrieval and ECMWF surface pressure is within 20 hPa, and retrieved reduced chi square of < 30) have been processed to retrieve XCO_2. Post-filtering checks for a successful retrieval outcome (a solution is converged upon in the full physics routine), and filters as detailed in Table 1 are applied. Note that Grad CO2 is defined as

$$\text{Grad CO}_2 = \left[1.00 \times 10^6\left(\text{CO}_2^{ret,S} - \text{CO}_2^{ret,700}\right) - \left(\text{CO}_2^{apr,S} - \text{CO}_2^{apr,700}\right)\right],$$

where $\text{CO}_2^{ret/apr,S}$ is the retrieved/a-priori CO_2 concentrations at the surface respectively, and $\text{CO}_2^{ret/apr,700}$ is the retrieved/a-priori CO_2 concentrations at 700hPa respectively. The factor in front of the CO_2^{ret} bracket converts CO_2^{ret} to ppm. This is not done for CO_2^{apr}. Delta Psurf (ΔP_{surf}) is defined as

$$\Delta P_{surf} = (P_{surf,ret} - P_{surf,apr}),$$

where $P_{surf,ret/apr}$ are the retrieved and a-priori surface pressures respectively.

Table 1. Product quality filter; retrievals that satisfy these criteria are marked as good.

Parameter	Acronym	Filter /min, max/
Retrieval changes of CO_2 gradient between 700hPa and surface	Grad CO_2	/-4.34, 21.47/
Retrieval changes on surface pressure from a-priori	ΔP_{surf}	/-4.45, 1.99/
Continuum correction coefficients of cos(x) of O_2 A band*	Continuum B1C3	/-0.76, 0.60/
Zero offset wavelength dependence slope of weak CO_2 band	Zeroff B2S	/-0.14, 0.017/
Surface albedo of CO_2 weak band	AlbedoB2	/0.033, 0.33/
Over water body (land fraction > 0.99 from L1B data)	-	Yes
Convergence in 10 iterations	-	Yes

*The detailed explanation is in the Algorithm Theoretical Basis Document Version 1 (ATBDv1), in section 4.2.3.6 Additional correction of the continuum, page 21.

3.3 Bias correction

For this data product, a bias correction is calculated and applied independently for each across-track footprint. The parameters for the bias correction are inferred from a multiple linear regression analysis of the difference between TanSat and TCCON XCO_2 observations for same the parameter P_i as used in post-screening (quality flags). The bias correction ($\Delta\mathrm{XCO}_2$) is calculated as follows:

$$\Delta\mathrm{XCO}_2 = \sum_{i=1}^{5} A_i \cdot P_i + B.$$

The bias-corrected XCO_2 (XCO_2^{corr}) is then given by:

$$\mathrm{XCO}_2^{corr} = \mathrm{XCO}_2^{ret} - \Delta\mathrm{XCO}_2$$

where XCO_2^{ret} is the XCO_2 as retrieved by UoL-FP. These parameters are selected by the rank of the XCO_2 error (individual difference to TCCON measurement) correlations (correlation coefficient). The coefficient A_i and offset B are optimized in the regression and used for bias correction of each individual retrieval. More details are given in Table 2.

Table 2. Bias correction coefficients. The coefficient for each row from left to right indicate the footprint.

Parameter1	Grad CO_2: The retrieval changes of layer CO_2 gradient between 700hPa and surface								
Coefficient1	0.094	0.096	0.082	0.094	0.099	0.123	0.123	0.130	0.083
Parameter2	ΔP_{surf}: The retrieval changes on surface pressure from a-priori								
Coefficient2	2.00	2.11	1.97	1.65	1.30	1.43	1.38	0.51	-0.027
Parameter3	Continuum B1C3: Continuum correction coefficients of cos(x) of O_2 A band								
Coefficient3	-0.31	-0.41	-0.47	-0.68	-0.41	0.20	-0.17	-0.88	-1.14
Parameter4	Zeroff B2S: Zero offset wavelength dependent-slope of CO_2 band								
Coefficient4	-2.02	-6.26	-11.41	-8.86	-0.80	-1.65	-3.65	-0.39	6.32
Parameter5	AlbedoB2: Surface albedo of CO_2 weak band								
Coefficient5	-11.48	-12.26	-12.97	-10.66	-5.81	-7.24	-9.26	-7.90	-4.85
Parameter6	Constant								
Coefficient6	1.08	1.19	1.38	1.31	0.84	0.92	0.91	0.77	0.92

3.4 Data Usage

The xco2_quality_flag variable must be applied to the data before use; a value of 0 indicates that the data has passed our quality control, while a value of 1 indicates that one filter in the quality control process has not passed. Soundings where more than one filter was not passed were excluded from the final dataset. All vertically resolved data is provided on levels (each layer surface as opposed to layers). This is especially important when applying UoL averaging kernels to model data.

3.5 Tools for Reading the Data

The data are stored in NetCDF (.nc) format, which can be read with standard tools.

3.6 Known Limitations and Issues

- As discussed in Section 3.3, we currently apply a bias correction to the data based upon a regression of geophysical parameters against the difference to the TCCON data.
- A preliminary comparison of our XCO_2 a posteriori error against the standard deviation of the TCCON-OCFP differences has indicated that our error estimates are in a similar range to the scatter of TCCON-OCFP differences but some outliers exist. Further exploration of this will be performed as part of the validation exercises.

3.7 Global data plots

This data release (CRDP#7) provides the entire publicly available TanSat dataset as processed by UoL-FP, spanning 1st March 2017 to 23rd May 2018, identified as CO2_TAN_OCFP v1.2. The CO2_TAN_OCFP v1.1 dataset provided global, land-only XCO2 retrievals spanning 1st March 2017 to 23rd May 2018. However, an error was detected in CO2_TAN_OCFP v1.1 where the filters and quality flags described in Section 3.2 were incorrectly applied to the data, necessitating the creation of CO2_TAN_OCFP v1.2.
This error is not present in the TCCON-only CO2_TAN_OCFP v1 data release, and only affects the CO2_TAN_OCFP v1.1 dataset. CO2_TAN_OCFP v1.2 (CRDP#7) corrects this error. The monthly median XCO_2 for March 2017 to May 2018 binned to 2x2 degree squares are plotted in Figure 3, and their corresponding standard deviations (the spread of the data for each bin) are plotted in Figure 4.

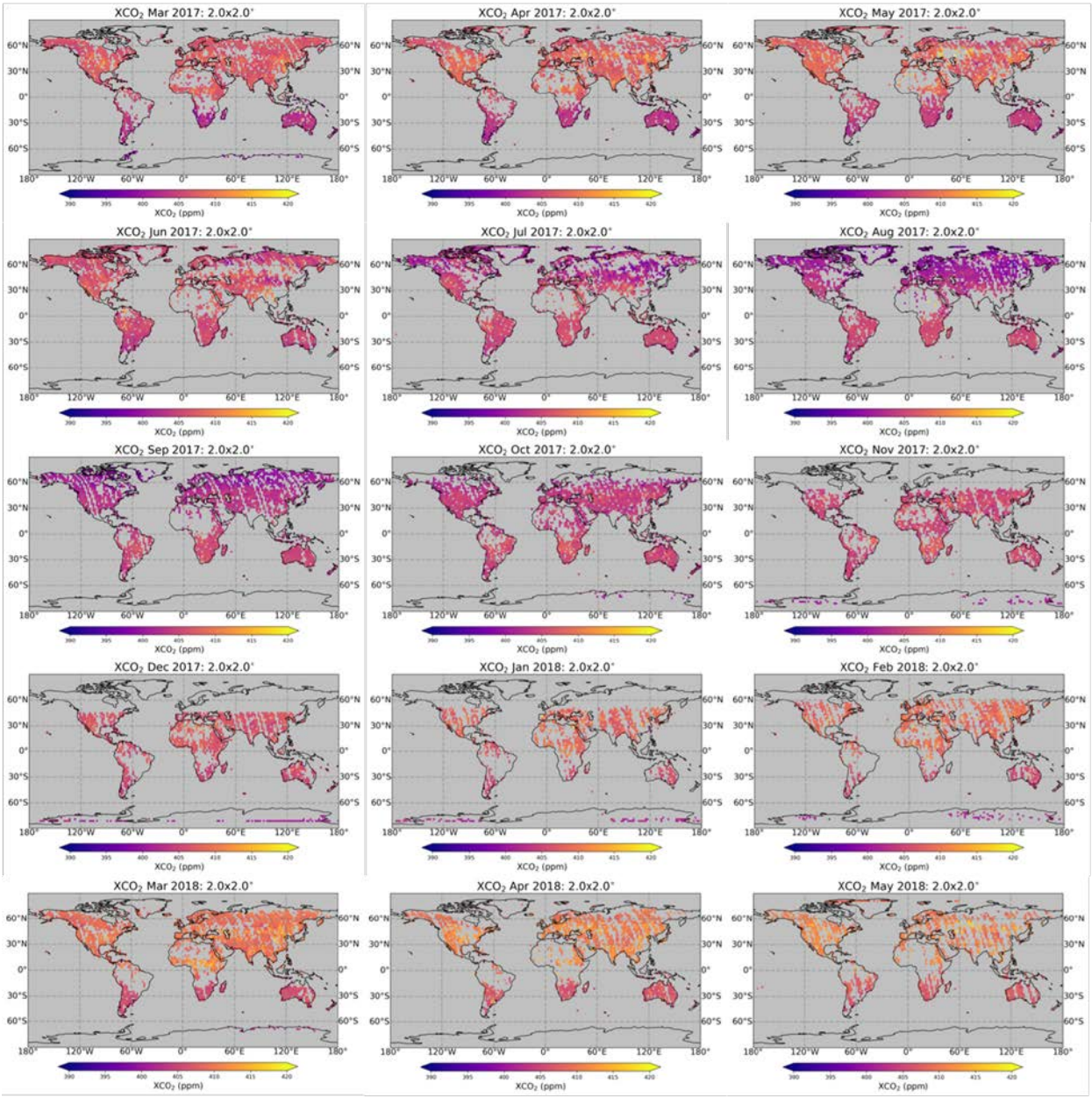

Figure 3: Global monthly median XCO_2 concentrations as a function of longitude and latitude for March 2017 – May 2018 as observed by TanSat. The soundings have been bias-corrected and filtered as per Table 1.

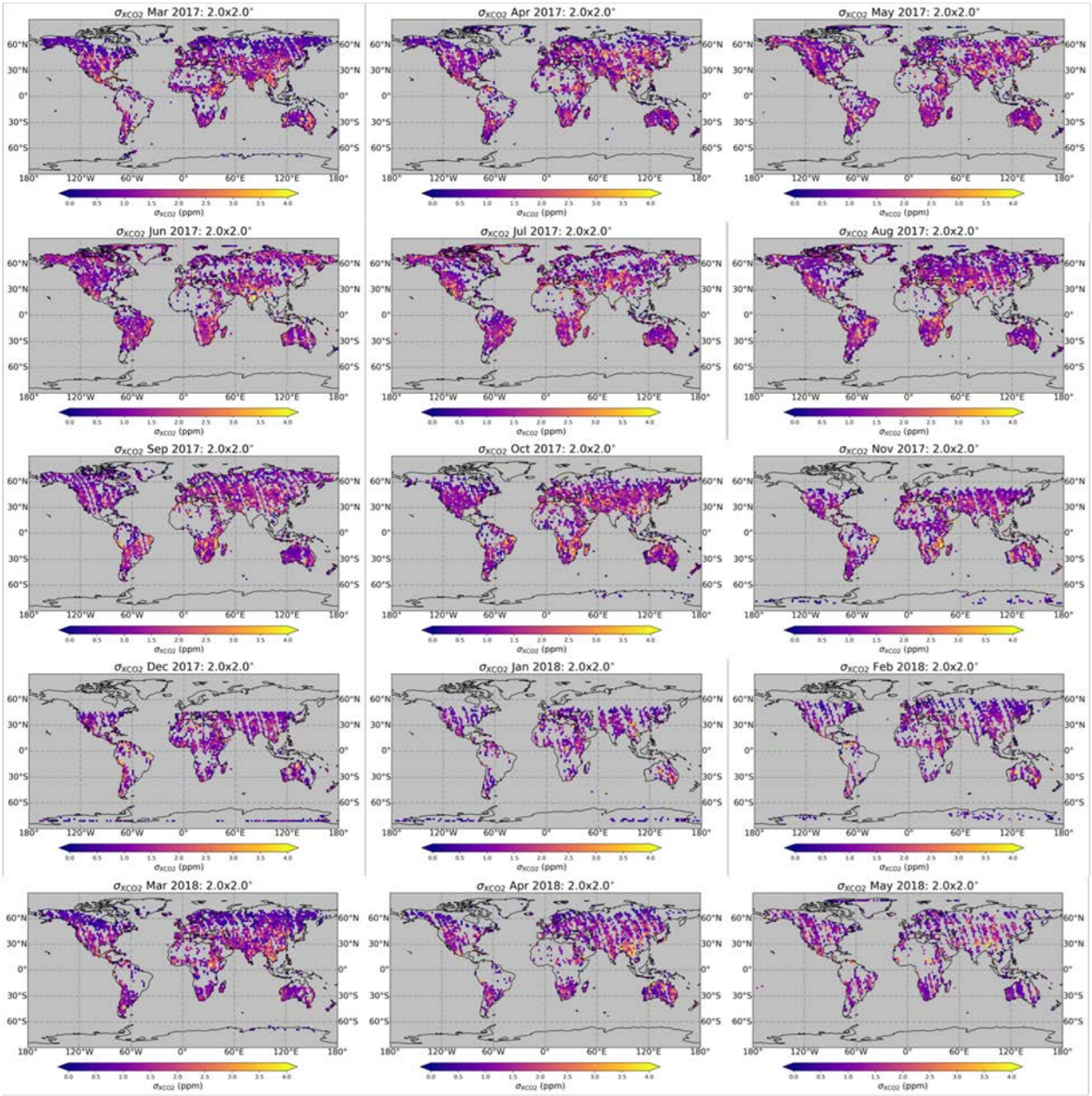

Figure 4: Standard deviation (σ_{XCO2}) of XCO_2 concentrations as a function of longitude and latitude for March 2017 – May 2018 as observed by TanSat. The soundings have been bias-corrected and filtered as per Table 1.

3.8 Data file content

NetCDF data files contain all of the common parameters for the ESA GHG-CCI data products (as outlined in the GHG-CCI Product Specification Document v4) as well as additional product specific parameters. A dimension of n refers to the number of retrievals per file, whilst a dimension of m refers to the number of levels retrieved for each sounding (typically 20).

Table 3. Common variables for the CO2_TAN_OCFP data product.

Name	Type	Dimensions	Units	Description
solar_zenith_angle	float	n	degree	Angle between line of sight to the sun and local vertical.
sensor_zenith_angle	float	n	degree	Angle between the line of sight to the sensor and the local vertical.
time	double	n	seconds since 1970-01-01 00:00:00	Measurement time.
longitude	float	n	degrees east	Centre longitude.
latitude	float	n	degrees north	Centre latitude.
pressure_levels	float	n, m	hPa	Vertical altitude coordinate in pressure units as used for averaging kernels.
pressure_weight	float	n, m		Pressure weights as used for averaging kernels.
xco2	float	n	1e-6	Retrieved column-averaged dry-air mole fraction of atmospheric CO_2 (XCO_2) in ppm. Bias correction applied.
xco2_no_bias_correction	float	n	1e-6	Retrieved column-averaged dry-air mole fraction of atmospheric CO_2 (XCO_2) in ppm. No bias correction applied.
xco2_uncertainty	float	n	1e-6	Statistical uncertainty of XCO_2 in ppm (1σ).
xco2_averaging_kernel	float	n, m		XCO_2 averaging kernel (a profile = vector for each single observation). Quantifies the altitude sensitivity of the XCO_2 retrieval.
co2_profile_apriori	float	n, m	1e-6	*A-priori* mole fraction profile of atmospheric CO_2 in ppm.
xco2_quality_flag	byte	n		Quality flag for XCO_2 retrieval, 0=good, 1=bad.

Table 4. Additional variables for the CO2_TAN_OCFP data product.

Name	Type	Dimensions	Units	Description
exposure_id	char	n, 17		Exposure identification number of the sounding.
surface_altitude	float	n	m	Altitude is the (geometric) height above the geoid, which is the reference geopotential surface, as derived from L1B data.
surface_altitude_stdev	float	n	m	Standard deviation of the surface elevation within the area of the TanSat sounding, as derived from L1B data.
surface_air_pressure_apriori	float	n	hPa	*A-priori* surface pressure value.
surface_air_pressure_apriori_std	float	n	hPa	*A-priori* surface pressure standard deviation.
gain	byte	n		TanSat has only one instrument gain mode. It is set to 1.
air_temperature_apriori	float	n, m	K	Air temperature is the bulk temperature of the air, not the surface (skin) temperature.
h2o_profile_apriori	float	n, m	ppm	*A-priori* mole fraction profile of atmospheric H_2O in ppm.
total_aod	float	n		Retrieved total aerosol optical depth.
aod_type1	float	n		Retrieved AOD type 1.
aod_type2	float	n		Retrieved AOD type 2.
cirrus	float	n		Retrieved AOD cirrus.
retr_flag	byte	n		Retrieval type flag (0 = land, 1 = glint).

4 Acknowledgement

We would like to thank International Reanalysis Cooperation on Carbon Satellites Data (IRCSD) and The Cooperation on the Analysis of carbon SAtellites data (CASA) who provided the TanSat L1B data through international collaboration.

5 References and Further Reading

/Boesch et al., 2011/ Boesch, H., D. Baker, B. Connor, D. Crisp, and C. Miller (2011), Global characterization of CO_2 column retrievals from shortwave-infrared satellite observations of the Orbiting Carbon Observatory-2 mission, Remote Sens., 3(2), 270-304, 2011

/Chevallier 2010/ Chevallier, F., P. Ciais, T. J. Conway, T. Aalto, B. E. Anderson, P. Bousquet, E. G. Brunke, L. Ciattaglia, Y. Esaki, M. Fröhlich, A.J. Gomez, A.J. Gomez-Pelaez, L. Haszpra, P. Krummel, R. Langenfelds, M. Leuenberger, T. Machida, F. Maignan, H. Matsueda, J. A. Morguí, H. Mukai, T. Nakazawa, P. Peylin, M. Ramonet, L. Rivier, Y. Sawa, M. Schmidt, P. Steele, S. A. Vay, A. T. Vermeulen, S. Wofsy, D. Worthy,2010: CO_2 surface fluxes at grid point scale estimated from a global 21-year reanalysis of atmospheric measurements. J. Geophys. Res., 115, D21307, doi:10.1029/2010JD013887

/Cogan 2012/ Cogan, A. J.*, Boesch, H., Parker, R.J., Feng, L., Palmer, P.I., Blavier, J.-F. L., Deutscher, N.M., Macatangay, R., Notholt, J., Roehl, C., Warneke, T., Wunch, D., 2012,* Atmospheric carbon dioxide retrieved from the Greenhouse gases Observing SATellite (GOSAT): Comparison with ground-based TCCON observations and GEOS-Chem model calculations*,* J. Geophys. Res.*,* 117*, D21301, doi:*10.1029/2012JD018087*.*

/Connor et al., 2008/ Connor, B. J., H. Boesch, G. Toon, B. Sen, C. Miller, and D. Crisp (2008), Orbiting Carbon Observatory: Inverse method and prospective error analysis, J. Geophys. Res., 113, D05305, doi:10.1029/2006JD008336.

/Kuze et al., 2009/ Kuze, A., H. Suto, M. Nakajima, and T. Hamazaki (2009), Thermal and near infrared sensor for carbon observation Fourier transform spectrometer on the greenhouse gases observing satellite for greenhouse gases monitoring, Applied Optics, 48(35), 6716-6733.

/Lin et al., 2017/ Lin C, Li C, Wang L, et al. Preflight spectral calibration of hyperspectral carbon dioxide spectrometer of TanSat (in Chinese). Opt Precision Eng, 25: 2064-2075, 2017.

/Liu et al., 2018/ Liu, Y., J. Wang, L. Yao, X. Chen, Z. Cai, D. Yang, Z. Yin, S. Gu, L. Tian, N. Lu, D. Lv, 2018: The TanSat mission: preliminary global observations. Sci. Bull., 63:1200-1207.

/Natraj et al., 2008/ Natraj, V., H. Boesch, R. J. D. Spurr, and Y. L. Yung (2008), Retrieval of XCO_2 from simulated Orbiting Carbon Observatory measurements using the fast linearized R-2OS radiative transfer model, Journal of Geophysical Research D: Atmospheres, 113(11).

/O'Dell et al., 2010/ O'Dell, C. W. (2010), Acceleration of multiple-scattering, hyper-spectral radiative transfer calculations via low-streams interpolation, Journal of Geophysical Research D: Atmospheres, 115(10).

/Saitoh et al., 2009/ Saitoh, N., R. Imasu, Y. Ota, and Y. Niwa (2009), CO_2 retrieval algorithm for the thermal infrared spectra of the greenhouse gases observing satellite: Potential of retrieving CO_2 vertical profile from high-resolution FTS sensor, Journal of Geophysical Research D: Atmospheres, 114(17).

/Spurr 2008/ Spurr, R. (2008). LIDORT and VLIDORT: Linearized pseudo-spherical scalar and vector discrete ordinate radiative transfer models for use in remote sensing retrieval problems. In Light Scattering Reviews 3 (pp. 229-275). Springer Berlin Heidelberg.

/Spurr et al., 2011/ Spurr, R., & Natraj, V. (2011). A linearized two-stream radiative transfer code for fast approximation of multiple-scatter fields. Journal of Quantitative Spectroscopy and Radiative Transfer, 112(16), 2630-2637.

/Yang et al., 2018/ Yang, D., Y. Liu, Z. Cai, X. Chen, L. Yao, and D. Lu, 2018: First Global Carbon Dioxide Maps Produced from TanSat Measurements. Adv. Atmos. Sci., 35(6), 621–623.

/Yang et al., 2020/ Yang, D. Boesch, H., Liu, Y., Somkuti, P., et al.: Toward high precision XCO2 retrieval on TanSat measurements: the retrieval improvement and validation against TCCON measurement. J. Geophys. Res. Atmos., 2020, 125, e2020JD032794.